Quantum yield limits for the detection of single-molecule fluorescence enhancement by a gold nanorod

Lu, X.; Ye, G.; Punj, D.; Chiechi, R.C.; Orrit, M.

Article

Quantum Yield Limits for the Detection of Single-Molecule Fluorescence Enhancement by a Gold Nanorod

Xuxing Lu, Gang Ye, Deep Punj, Ryan C. Chiechi,* and Michel Orrit*

Read Online

ACCESS | Metrics & More | Article Recommendations | SI Supporting Information

ABSTRACT: Fluorescence-based single-molecule optical detection techniques are widely chosen over other methods, owing to the ease of background screening and better signal-to-noise throughput. Nonetheless, the methodology still suffers from limitations imposed by weak emitting properties of most molecules. Plasmonic nanostructures, such as gold nanorods, can significantly enhance the fluorescence signal of a weak emitter, extending the application of these techniques to a wider range of species. In this work, we explore the lower limit of fluorescence quantum yield for single-molecule detection, using a single gold nanorod to enhance molecular fluorescence. We specifically designed an infrared dye with the extremely low quantum yield of 10^{-4} and a comparatively large Stokes shift of 3000 cm^{-1} to demonstrate single-molecule detection by fluorescence enhancement. This example allows us to discuss more general cases. We estimate theoretically the optimal excitation wavelength and the plasmon resonance of the rod that maximize the fluorescence signals. We then confirm experimentally the detection of single-molecule fluorescence with an enhancement factor of 3 orders of magnitude for the quantum yield 10^{-4}. Theoretical simulations indicate that single-molecule signals should be detectable for molecules with quantum yield as low as 10^{-6}, provided the dwell time of the molecules in the plasmonic hot spot is long enough.

KEYWORDS: *plasmonics, gold nanorod, single-molecule detection, low quantum yields, fluorescence enhancement, signal-to-noise ratio*
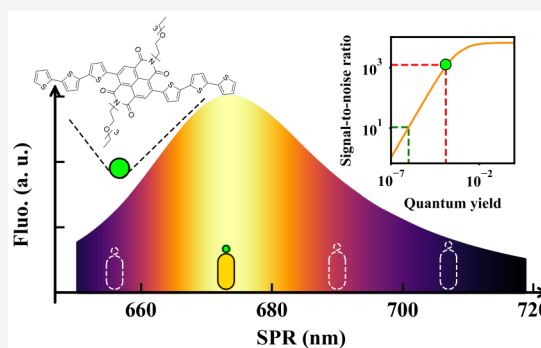
O ptical detection of single molecules lies at the core of numerous biochemical studies as it opens up the possibility of investigating individual molecular behavior usually hidden in the ensemble measurements.[1−5] The key to successful single-molecule detection is to optimize and extract a weak signal from a high background.[6−9] Over the past decades, fluorescence-based single-molecule techniques have been widely applied due to the easy but efficient background suppression and their high sensitivity.[9−14] In this method, the photons emitted at a longer wavelength than the excitation light (Stokes-shifted) can easily be discriminated from the background by spectral filtering, providing exceptional contrast and thereby enabling the detection and study of weak single-molecule signals.[14,15] Notwithstanding the many successes of fluorescence-based single-molecule techniques, it would be important to extend them to a broader range of absorbing molecules with weak emission, especially those emitting in the near-infrared. Chen et al.[16] have designed deep-red low quantum yield dyes (quantum yield ≈ 0.002) with a large Stokes shift that prove to be better in staining mitochondria than normal MitoTrackers. In another work, water-soluble low quantum yield rylene derivative dyes (quantum yield ≈ 0.01) were studied for the application of membrane labeling.[17] They prove to be more photostable than other well-established dyes. While dealing with low-quantum-yield dyes, conventional spectrofluorimeters cannot be effectively used to study single-molecule fluorescence, mainly because impurities become dominant. The decrease in quantum efficiency for red and NIR dyes is usually attributed to the energy gap law.[18] Recently, the low quantum yield of red fluorescent proteins has been attributed to the presence of dark chromophores,[19] which limit their sensing applications.[20,21] One way to improve these weak emitters is to minimize their nonradiative decay. Another promising strategy to improve the fluorescence efficiency of single-molecule fluorescence is to enhance the radiative emission rate by coupling the fluorophores to plasmonic structures, which can enhance the local field by confining the electromagnetic energy to volumes well below the diffraction limit.[2,13,22−26]

Compared to strong emitters, poor emitters with low quantum yields benefit from a stronger fluorescence enhancement by plasmonic structures. They are easier to detect at the single-molecule level because of reduced background from unenhanced molecules. This has led researchers in previous
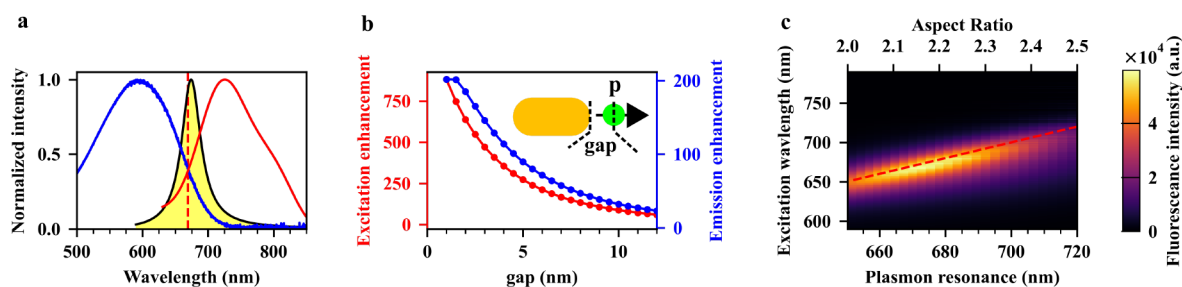
Figure 1. (a) Absorption (blue) and emission (red) spectra of NDI-2TEG-3T in toluene. The shaded band is the gold nanorod scattering spectrum calculated for the aspect ratio corresponding to the optimum normalized intensity (see (c)) at an excitation wavelength of 671 nm (vertical red dashed line). (b) Calculated excitation (red) and emission (blue) enhancements as functions of the gap, that is, the separation of the molecule from the tip of the gold nanorod (inset: schematic of the simulated molecule-nanorod system). (c) Estimated enhanced fluorescence intensity as a function of the excitation wavelength and of the plasmon resonance wavelength of the gold nanorod. The fluorescence intensity was normalized by the nonenhanced intensity of the fluorescence excited at 671 nm. The red dashed straight line corresponds to the molecule being excited at the wavelength of the plasmon resonance. All values are obtained by varying the gap and selecting the gap value providing maximum enhancement.

studies to employ quenching agents such as methyl viologen[27−29] and nickel chloride[30] to reduce the quantum yield of the emitter. The plasmonic structures in those experiments were fabricated by various top-down and bottom-up approaches. Fluorescence enhancement of emitters with a quantum yield down to 1×10^{-3} has been experimentally demonstrated with nanofabricated bow-tie antennas.[31,32] More convenient alternative plasmonic structures are wet-chemically synthesized gold nanorods (GNRs), which have attracted significant interest for their facile synthesis and unique optical properties.[25,33−35] The collective oscillations of the GNR's free electrons, known as localized surface plasmons, strongly confine the electromagnetic field into a subwavelength region near the tips, thereby enhancing the excitation rates of the molecules nearby.[24] The plasmonic resonance of GNRs can easily be tuned from the red to the near-infrared range by adjusting their aspect ratio, making them a good single-molecule detection platform for a wide range of fluorescent species.[25] In addition to the excitation enhancement, GNR can enhance radiative channels by increasing the local density of photon states. However, this enhancement of spontaneous emission is generally accompanied by enhanced nonradiative decay channels. Going closer to the metal will generally increase the excitation and radiative enhancements, but at the same time, it will also increase the nonradiative processes responsible for fluorescence quenching, leading to an optimal range for the total enhancement.[36−38] Overlapping the excitation wavelength and the plasmon resonance with the emission spectra of a particular emitter can enhance both the excitation and emission rates, thereby improving the fluorescence enhancement. By using this strategy, we have earlier reported the detection of gold-nanorod-enhanced single-molecule fluorescence from dyes with a quantum yield of 10^{-3}, with an enhancement factor of up to 1000.[25] In the present work, we explore the possibility to enhance the fluorescence of dyes with even lower quantum yield, while keeping the fluorescence observable against background, the strongest source of which is the intrinsic photoluminescence of gold, also enhanced by the plasmon resonance. When going to weaker quantum yields, it is not enough to consider the enhancement factor alone. Indeed, the quantity determining the detection limit is the signal-to-noise ratio, which depends in a complex manner on the plasmon enhancement, the molecular absorption cross section and the fluorescence quantum yield. Therefore, we undertook careful

theoretical and experimental investigations of fluorescence enhancement for weak quantum yields in view of optimizing the enhanced fluorescence signal and of extending single-molecule techniques to a much broader range of emitting species.

In this study, we explore single-molecule detection of very weak emitters with quantum yields as low as 1×10^{-4}, by enhancing their fluorescence with a single gold nanorod. To optimize the signal, we need to consider the molecule's Stokes shift (about 150 nm or 3000 cm^{-1}). Indeed, we have a trade-off between molecular excitation rate and the fluorescence enhancement. Using theoretical simulations, we optimize the excitation wavelength and the plasmon resonance of the rod. We then apply these parameters to detect single-molecule fluorescence experimentally with enhancement factors of 3 orders of magnitude. We further investigate the quantum yield dependence of the signal-to-noise ratio of the plasmon-emitter coupled system and estimate the lowest quantum yield for which single emitters can be detected in the near field of a single gold nanorod. Although we consider only single nanorods here because of their ease of synthesis, modeling, and manipulation, our results can easily be extended to more complicated nanostructures with much higher near-field enhancement, such as strongly coupled gold nanoparticle dimers or clusters.

■ RESULTS AND DISCUSSION

In this work, instead of selecting molecules with small Stokes shifts (i.e., separation between the maxima of absorption and emission) as done in previous studies,[25] we focus on the case of low-quantum-yield dyes, which often have much larger Stokes shifts. For large Stokes shifts (i.e., for small overlaps between the absorption and emission spectra), enhancing both the excitation and the radiation processes with the same narrow-band GNR antenna is very difficult. As a consequence, detection of such single molecules becomes harder than those with small Stokes shifts. To get maximum signals, we will have to sacrifice a fraction of the enhancement factor. In a simple coupled system of a single gold nanorod and an emitter, we can optimize emission by balancing excitation and radiative enhancements, through adjustment of the excitation wavelength and of the aspect ratio of the gold nanorod.

For our study, we selected a molecule of the donor−acceptor type based on naphthalene diimide-terthiophene (NDI-2TEG-3T) because it is a very weak emitter. It has a

measured quantum yield of about 1.3×10^{-4} and has a large Stokes shift between the emission and the absorption bands. The structure of the molecule is shown in the inset of Figure 2c, and the synthesis details are given in the Supporting Information. The low fluorescence efficiency of NDI-2TEG-3T is due to its typical donor−acceptor structure. The introduction of terthiophene units as donors provides an energy level that is suitable for the photoinduced electron transfer process. This extra channel for nonradiative exciton relaxation consequently quenches the fluorescence.[39,40] When measured in toluene, the NDI-2TEG-3T molecule shows two distinct absorption bands. One of these two bands is assigned to a high-energy $\pi-\pi^*$ transition in the range of 300 to 400 nm. The second one is a low-energy broad intramolecular charge-transfer transition in the range of 500 to 700 nm with its maximum at 590 nm. It originates from the electron-rich terthiophene group to the electron-deficient NDI unit. We focus on the second band with the maximum at 590 nm as it overlaps better with typical gold nanorod resonances. The fluorescence band lies in the near-infrared range with its maximum at about 740 nm. Both bands can be overlapped with the plasmon resonance of gold nanorods, opening possibilities of very large fluorescence enhancements through the combination of excitation and emission enhancements. However, as mentioned before, we need to explore the dependence of the enhanced fluorescence signal on excitation wavelength and on plasmon resonance in order to optimize it.

We begin our discussion with the simulation of fluorescence enhancement of NDI-2TEG-3T by a single gold nanorod. For simplicity, we consider the molecule to lie on the long symmetry axis of the rod, at a variable distance from the tip (we call this distance the "gap" as represented in the inset of Figure 1b). Considering the small quantum yield and the short lifetime of NDI-2TEG-3T molecules, we apply the simplified two-level scheme model for the calculation of the fluorescence enhancement factor, which neglects the excitation saturation (see Supporting Information for more details). Moreover, we assume both the excitation wave polarization and the molecular dipole to be oriented along the same longitudinal nanorod axis. This simulation therefore applies to the configuration providing maximum enhancement. The plasmon wavelength of the nanorod was tuned by changing its length while keeping its diameter constant at 25 nm, which is the average rod diameter in our experiments. The dielectric permittivity of gold was taken from Johnson and Christy,[41] and the refractive index of the medium was set to 1.496 for toluene.

Figure 1b shows the dependence of the excitation and emission enhancements on the gap, with the excitation and plasmon wavelengths at 671 and 673 nm, respectively. The excitation enhancement increases monotonously as the gap decreases. The emission enhancement, however, presents a maximum, found here at the gap of about $d_m = 1.5$ nm. The maximum emission enhancement reaches about 200, leading to a maximum total enhancement of 5 orders of magnitude. The value of d_m depends on the dye quantum yield. For quantum yields such as 1×10^{-2}, the optimal gap is about 4 nm (see Figure S11), whereas for very low quantum yields, the optimal gap shifts to values of 1.5 nm or less (1.5 nm for a yield of 1.3×10^{-4} in Figure 1b). This is because, by reducing the gap, we can benefit from higher excitation and radiative enhancements, while quenching by the metal is still dominated by nonradiative relaxation within the molecule. Here, we should keep in mind that if the molecule is too close to the gold surface

(e.g., in the scale of Å), the point dipole model is no longer valid. In this case, full quantum mechanical calculations would be needed to get the proper enhancement values by the gold nanorod, taking into account the chemical structure of the molecule and its interaction with the gold. As a consequence, we keep the minimum gap as 1 nm in all the simulations.

Next, we optimized the fluorescence intensity of the nanorod−molecule system, by varying both the excitation wavelength and the aspect ratio of the gold nanorod. Figure 1c gives the normalized fluorescence intensity as a function of the excitation wavelength and of the resonance wavelength of the gold nanorod. To obtain this plot, we have varied the gap value to optimize the intensity, for each excitation and plasmon wavelength. The plot is given for a fixed quantum yield of 1.3×10^{-4}, corresponding to NDI-2TEG-3T in toluene. As can be seen on Figure 1c, the maximum fluorescence intensity enhanced by each rod is obtained for excitation nearly in resonance with the plasmon, that is, $(\omega_{exc} \sim \omega_{sp})$, because most of the enhancement arises from the excitation. Here ω_{exc} is the frequency of the excitation light source and ω_{sp} is the frequency of the surface plasmon resonance. Next, we note an intensity maximum (sweet spot) at the plasmon wavelength of about 674 nm, which balances the enhancement of both excitation and radiative processes. The total fluorescence enhancement value at this spot is 50000 times. Here, we can see in Figure 1a that the plasmon resonance at the sweet spot (yellow shaded band) does not overlap exactly with the emission maximum of the molecule, as had been postulated in previous studies to give maximum total fluorescence enhancement (see Supporting Information), but corresponds to the maximum overlap with both the dye absorption (blue line) and emission (red line) spectrum.

We can interpret the results of simulations in Figure 1c in a very simple way. We notice that the total intensity in eq S10 is a product of the molecular absorption cross section C_{abs}, the excitation enhancement factor, and the emission enhancement, which is nearly equal to the radiative enhancement factor in the limit of very weak quantum yields. As the excitation and radiation processes are both enhanced by the same narrow plasmon resonance (Lorentzian form), we can approximate the enhanced intensity as

$$I(\omega_{exc}) \propto C_{abs}(\omega_{exc}) \cdot F_{dye}(\omega_{exc}) \cdot f(\omega_{exc}) \qquad (1)$$

which means we tune the plasmon resonance and the excitation wavelength to the maximum overlap between absorption and emission of the molecule (see extensive mathematical justification in the Supporting Information).

We performed fluorescence enhancement experiments on NDI-2TEG-3T molecules under the theoretically derived optimum conditions. Gold nanorods, with average plasmon wavelength of 614 nm, were immobilized on the surface of clean coverslips and immersed in toluene containing different concentrations of NDI-2TEG-3T. The plasmon wavelength of the gold nanorod red-shifts to about 680 nm in toluene due to its high refractive index of 1.496. The measurements were performed on a home-built confocal microscope setup. A circularly polarized continuous-wave (CW) laser with the wavelength of 671 nm was chosen as the excitation source and was focused by an oil immersion objective with a numerical aperture (NA) of 1.4 to a diffraction-limited spot (about 0.5 μm in diameter). A long-pass filter (≥675 nm LongPass U-Grade 671/RazorEdge, Semrock) was used to separate the fluorescence signal from the background of scattered laser
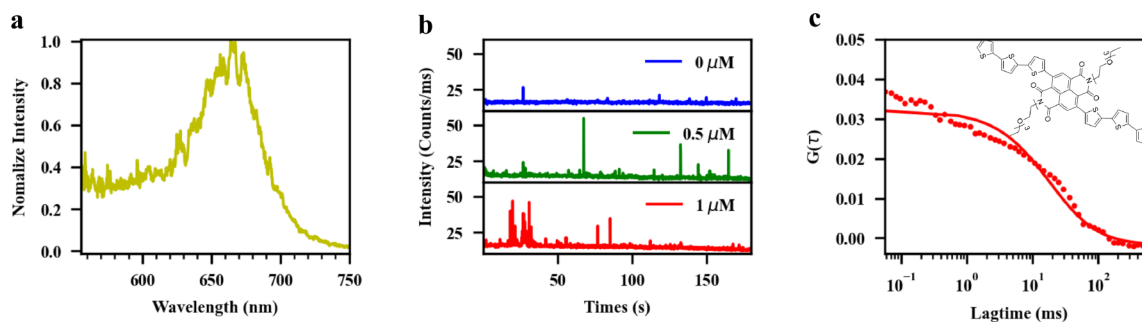
Figure 2. (a) Photoluminescence spectra of the gold nanorod deposited on a glass surface and immersed in toluene, which was used to enhance the fluorescence of NDI-2TEG-3T. (b) Photoluminescence time trace from the single gold nanorod immersed in a solution of NDI-2TEG-3T in toluene with different concentrations. (c) The measured (red dashed line) autocorrelation curve of the fluorescence bursts shown in (b) for molecular concentration of 1 μM and the single exponential fitting of the curve (red solid line). Inset: chemical structure of NDI-2TEG-3T.

light. Before adding the NDI-2TEG-3T solution, we recorded photoluminescence (PL) spectra of each bright spot to make sure that the nanoparticle under study had the single Lorentzian line shape of a single gold nanorod. Time traces were taken for each nanorod under different concentrations of the molecules while keeping the excitation power constant. In each step, the concentration of the molecules was adjusted by adding a certain amount of high concentrated NDI-2TEG-3T solution (50 μM) sequentially, followed by some 10 min for diffusion to homogenize the concentration. As confirmed by bulk measurements of the concentration-dependent absorbance, NDI-2TEG-3T is very well dissolved in toluene in our experimental range of molecular concentration (see Figure S5). The absence of spectral signatures from dimers and higher clusters confirms that the molecules are well separated from each other, and hence access the plasmonic hot spot independently of each other.

Figure 2 shows typical experimental measurements of single-molecule fluorescence enhanced by a single gold nanorod. We first identify single nanorods among spots in the optical image from their photoluminescence spectrum, which has a Lorentzian shape and is relatively narrow. Figure 2a indicates a single nanorod with its plasmon resonance at 667 nm. In the intensity time traces, as shown in Figure 2b, the background arises from gold nanorod photoluminescence and from the very weak nonenhanced fluorescence of all the molecules in the volume of the excitation focal spot, while the bursts are due to the enhanced fluorescence of the molecules within the hot spots near the tips of the rod. To verify that the bursts indeed arise from single molecules, we compared the time traces taken at different NDI-2TEG-3T concentrations. As shown in Figure 2b, in pure toluene solvent, we do not see any strong bursts in the fluorescence time-trace. Bursts appear more and more frequently in the time traces as we increase the NDI-2TEG-3T concentration, while the background remains at a similar level. This observation confirms that the signal from all the nonenhanced molecules in the focal spot (about 52 molecules) is negligible compared to the photoluminescence of the rod, even though the molecular concentration is as high as 1.0 μM, because the quantum yield of NDI-2TEG-3T is exceedingly weak. The bursts arise from molecules diffusing through, or being transiently stuck in, the tiny hot spots near the tips of the nanorods. The probability of such bursts increases as the molecular concentration increases. By analyzing the highest bursts in the fluorescence time trace, we see the typical single-step single molecule bursts with the time duration in the order of 10 ms (Figure S9), which confirms that only a single

molecule was present in the hotspot during the burst and indicated that it was transiently immobilized. The autocorrelation curve for the fluorescence bursts corresponding to molar concentration of 1 μM is shown in Figure 2c. By fitting the autocorrelation curve to a single exponential, we obtained an average correlation time of 27 ms, which is obviously too long to be due to the free diffusion of molecules through the near field of a nanorod according to the previous works,[24−26] where passivation of the glass surface completely suppressed the long-lived bursts. The correlation time results from an interplay between sticking time and bleaching time in the experimental conditions. Here, it can most likely be considered as the result of the transient sticking of dye molecules. Noting that sticking to the metal surface would lead to complete quenching of the fluorescence,[42−44] we assign the long bursts to sticking onto the glass substrate. The intensities of the bursts in the time traces depend on the orientation and spatial position of the molecules with respect to the gold nanorods during their residence within the hot spot. As an approximation, we represented the maximum enhanced fluorescence as the largest intensity of the bursts in the time trace, subtracting the background.[45] Those maximum bursts are around 55 counts/ms, whereas the background is 16 counts/ms. To get the enhancement factor, we evaluated the fluorescence signal of one NDI-2TEG-3T molecule from a high-concentration solution (50 μM) by recording the fluorescence signal under the same experimental conditions but on an area without a nanorod. Figure S7 (of the Supporting Information) shows such a trace with an average count of 36 per 1 ms bin time when the excitation power is 3.3× larger than the power we used for single molecule measurements. We estimate the number of molecules in the focal volume (about 0.061 fL) at the given concentration of 50 μM to be about 1800 at any given time. From this we get an estimate of the average intensity of about 6 ± 1 counts/s per molecule. This corresponds to an enhancement factor of about 6500. Taking into account the circularly polarized excitation in the experiment, the enhancement factor will become 13000 if the gold nanorod is excited by a laser with the polarization along its long axis. Note that with the enhanced signal being stochastic, we estimate it by the largest observed signal, which entails an error of roughly a factor of 2. The obtained enhancement value is significantly lower than the best enhancement factor expected for this low quantum yield (more than 100000, see Figure 3a hereafter). Various factors can explain the difference: (i) the plasmon resonance was not perfectly tuned to the laser and dye wavelengths; (ii) the
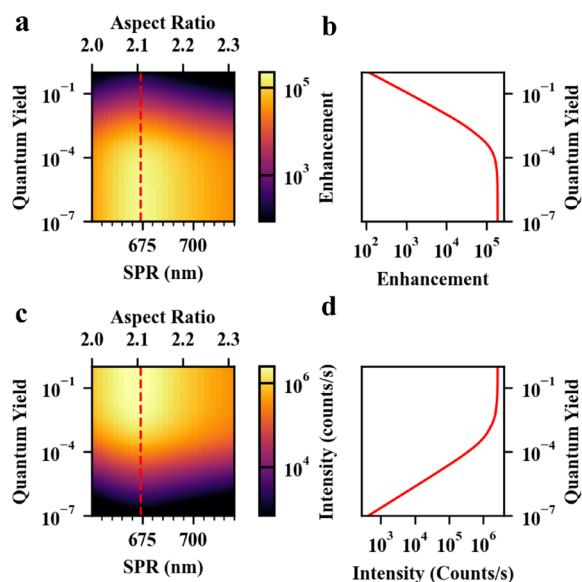
Figure 3. (a, c) Simulated fluorescence enhancement (a) and the estimated photon counts (c) from emitters with different quantum yields as functions of the plasmon resonance of the gold nanorod. The excitation wavelength was set as 671 nm. (b, d) Corresponding enhancement factor and emitted intensity enhanced by a gold nanorod with the optimized plasmon wavelength of 673 nm (dashed red lines in a and c) as functions of the quantum yield of the molecule. In this plot, we kept the molecular absorption cross section and the excitation intensity constant, that is, equal to the intensity used in the NDI-2TEG-3T measurements.

orientation of the molecule was probably not optimal as chosen in the calculation; and, most importantly, (iii) the position of the dye was probably on the glass slide and not along the rod axis, which is the best position for enhancement. The latter factor can lead to a significant reduction in the enhancement factor.[46]

To illustrate how the enhancement factor can been tuned by the plasmon resonance of gold nanorods, we examined the fluorescence time traces recorded on gold nanorods with different plasmon wavelengths (see Figure S10). We can see that, as the SPR of the gold nanorods is detuned from the laser (blue shift from 667 to 638 nm), the strongest fluorescence bursts in the time traces are decreasing, with the enhancement factors decreasing from about 6500 to about 2000, respectively.

According to the aforementioned studies, we learn that, by properly choosing the wavelengths of the excitation light and the plasmon resonance, we are able to detect single-molecule fluorescence enhanced by a single gold nanorod with high signal-to-background ratio, even though the molecular quantum yield is as low as 1.3×10^{-4}. To gain further insight into the possibility of fluorescence enhancement of single molecules with a simple individual gold nanorod, we performed numerical simulations of the detection limit for molecules with very low quantum yields, keeping the same molecular absorption cross section as NDI-2TEG-3T. In this study, we must consider which background sources will compete with enhanced fluorescence and prevent the detection of single events. Neglecting experimental imperfections, two sources of background as intrinsic to the sample under study: (i) Fluorescence of molecules out of the hot spot. Although the concentration of molecules can exceed a micromolar, their fluorescence is negligible (less than 300 cps) because of the

dye's low quantum yield. (ii) Photoluminescence of the gold nanorod itself. Although intrinsic gold photoluminescence is very weak (10^{-10}),[47] the photoluminescence signal is also enhanced by the plasmon resonance and cannot be separated from the enhanced fluorescence. A typical PL rate for the NRs in this study was 10 kcps. We therefore base our discussion of the signal-to-background ratio on this value.

Figure 3 gives the simulated single-molecule fluorescence enhancement by a single gold nanorod as a function of molecular quantum yield. For the sake of comparison, we used the same excitation wavelength 671 nm, the same absorption cross section, and the same fluorescence spectrum as those of NDI-2TEG-3T we used in our measurements. Therefore, the enhanced radiative and metal-induced nonradiative rates are independent of the quantum yields, and they share the same spectral dependence on the plasmon resonance. Because the spectral dependence of the plasmon-dependent emission enhancement is not changed, the spectral position of the plasmon resonance with maximum enhancement is conserved, independently of the quantum yield (see eq S9). As shown in Figure 3a,c, the spectral position of the maximum enhancement factor and of the maximum enhanced fluorescence intensity do not change for different quantum yields. All are located at 674 nm (dashed red line in Figure 3a,c). At the optimal plasmon wavelength of 674 nm, the total enhancement factor increases dramatically at first, as the quantum yield of the emitter decreases (see Figure 3d), until it approaches the constant value of 2×10^5, which confirms the simple expression in eq S21 for the emission enhancement limit. To understand this result, we approximate the product of excitation and radiative enhancements $\xi_{exc} \times \xi_{rad}$ (i.e., the total fluorescence enhancement factor expected for vanishing quantum yield) as the fourth power of the field enhancement factor: $\xi_{total} \xrightarrow{\eta_0 \to 0} \xi_{ext} \cdot \xi_{rad} \propto |E/E_0|^2 \cdot |E/E_0|^2 \sim |E/E_0|^4$, the value of which is $(27)^4 \sim 5 \times 10^5$. The enhanced fluorescence intensity, however, drops with the quantum yield, as can be seen by substituting eq S9 into eq S10. The enhanced intensity (see Figure 3d) at first is approximately constant down to a quantum yield of about 10^{-3}, as the decrease in molecular quantum yield is roughly compensated by an associated increase in enhancement. However, when the molecular quantum yield becomes lower than 10^{-3}, the enhancement factor saturates, causing the intensity to drop with the molecular quantum yield. As shown in Figure 3d, the estimated photon intensity from a single emitter drops from 2×10^6 counts/s to 4×10^3 counts/s when its quantum yield η_0 decreases from 100% to 10^{-6}. Such a signal would still be detectable above the photoluminescence background of the nanorod, even for an integration time as short as 10 ms.

From the above discussion, we find that by enhancing the fluorescence with a single gold nanorod, one can expect photon intensities of thousands of counts/s from a single molecule, even though its quantum yield is as low as 10^{-6}, a single-molecule fluorescence comparable with the background from the luminescence of a single gold nanorod ($\sim 10^4$ counts/s), under typical excitation laser power in the experiments. However, sufficiently long integration times are needed (about 10 ms), which require a high medium viscosity or transient sticking of the molecules. In principle, this contrast allows us to detect the signal from a single molecule. By looking at the signal-to-noise ratio in Figure 4, we can see that $SNR \sim 10$ for molecules with the quantum yield of 10^{-6} (green dashed), and
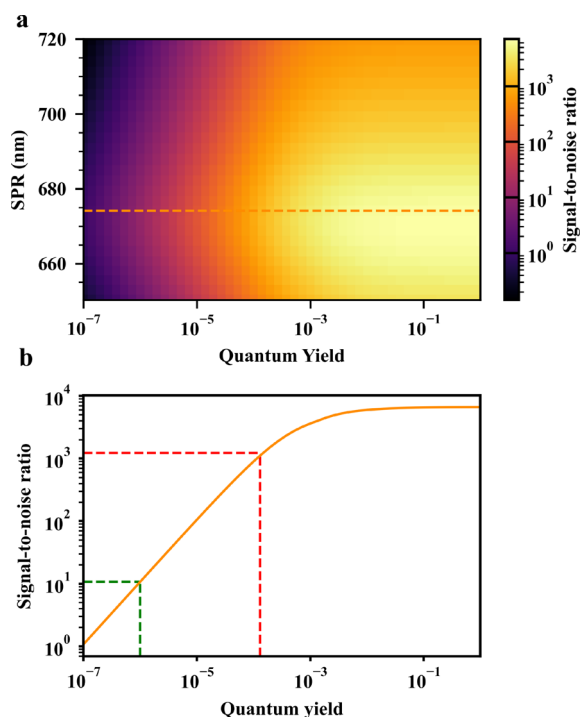
Figure 4. (a) Signal-to-noise ratio of the coupled nanorod-molecule system with different plamsonic resonance as functions of the molecular quantum yields. (b) Corresponding signal-to-noise ratio with the excitation wavelength at 671 nm and the plasmon resonance of the gold nanorod optimizing for the properties of NDI-2TEG-3T (dashed orange line in (a)). We assumed a typical experimental background of nanorod photoluminescence (10^4 cps) at the plasmonic wavelengh of 673 nm, and the photoluminescence of other plasmonic wavelengths were normalized by their scattering cross sections. Integration time was set as 0.1 s. The green dashed line corresponds to molecule of quantum yield 10^{-6} and the red dashed line corresponds to the quantum yield of NDI-2TEG-3T molecule (1.3×10^{-4}).

Figure 5. Color plots of the calculated fluorescence enhancement (a) and of the estimated photon intensity (b) as functions of the separation of the rod tip to emitter distance (gap) and of the emitter's quantum yield. The green dashed lines in each figure are contours of equal enhancements and intensities. All molecular parameters except the yield were kept constant, as above.

even though it is 100× smaller than that of the measured NDI-2TEG-3T molecules with the quantum yield of 1.3×10^{-4} (red dashed), it still provides enough contrast to distinguish single-molecule signals from background noise.

Following the above discussion, one should keep in mind that, as the quantum yield decreases, the volume for the single-molecule fluorescence to be effectively enhanced will also decrease. This can be understood intuitively. As we reduce the quantum yield of the molecule, internal conversion will outcompete quenching by the metal at shorter and shorter distance, so that the molecules can get closer to the gold nanorod and reach larger fluorescence enhancement. This increase of the enhancement can mitigate, to some extent, the strong fluorescence reduction due to the decreasing quantum yield. This partial compensation is seen clearly on the green dashed lines in Figure 5, which scales more favorably than quantum yield for small gaps. Therefore, the molecules with a smaller quantum yield can get closer to the tips of the nanorod to emit more photons. As a consequence, because diffusion time scales as the squared distance, successful detection of single molecules with very small quantum yield requires slower diffusion or longer binding events than molecule with high quantum yields. Moreover, the reduced effective near-field volume leads to a lower number of detected events, which can be compensated by increasing the concentration of the

molecules. We made use of this compensation in our experiment, as we used molecular concentrations in the μM range instead of nM, as was done in the previous work with quantum yield of 10^{-2}. Additionally, we could also make sure to keep the molecules for longer times in the vicinity of the nanorod tips. This can be done either by slowing down the molecular diffusion in a more viscous solvent, or by transient binding of the molecules within the effective near-field volume, for example, through DNA-transient binding.[48]

In conclusion, we have provided a detailed study of single-molecule fluorescence enhancement by wet-chemically synthesized single gold nanorods, for extremely weak emitters. The molecule we studied, NDI-2TEG-3T, was specifically designed to emit in the near-infrared range, but with a very low quantum yield of 1×10^{-4}, and a large Stokes shift of 150 nm. Our work provides a suitable demonstration of single-molecule fluorescence enhancement by a single gold nanorod. Our numerical simulations show that, in order to optimize count rates from molecules with low quantum yield and large Stokes shift, we need to optimize the excitation wavelength and the plasmon resonance of the gold nanorod. Based on our theoretical study, we successfully detected single-molecule fluorescence bursts with enhancement factors of up to 10^4 with a simple gold nanorod. The squeezing of the effective near-field volume for enhancement of low-quantum-yield dyes allows us to detect single-molecule signals from solutions of high molecular concentrations, in the range of μM, with high contrast. Theoretical analysis further shows that even for quantum yields as low as 10^{-6}, we will still be able to detect single molecules by fluorescence enhancement by a single gold nanorod, provided the residence time in the effective near-field is longer than tens of ms. The experimental method and the theoretical model presented in this work can be readily extended to other plasmonic nanostructures, which may promote single-molecule techniques based on fluorescence enhancement to a wider range of applications.

■ ASSOCIATED CONTENT

ⓢ Supporting Information

The Supporting Information is available free of charge at https://pubs.acs.org/doi/10.1021/acsphotonics.0c00803.

> Synthesis and characterization of NDI-2TEG-3T, fluorescence of NDI-2TEG-3T in bulk, single-molecule fluorescence of NDI-2TEG-3T enhanced by a gold nanorod, fluorescence enhancement simulations, and a dual-Lorentzian model for the fluorescence enhancement by a gold nanorod (PDF)

■ AUTHOR INFORMATION

Corresponding Authors

Ryan C. Chiechi − *Stratingh Institute for Chemistry, Zernike Institute for Advanced Materials, University of Groningen, 9747 AG Groningen, Netherlands;* ⓞ orcid.org/0000-0002-0895-2095; Email: r.c.chiechi@rug.nl

Michel Orrit − *Huygens-Kamerlingh Onnes Laboratory, Leiden University, 2300 RA Leiden, Netherlands;* ⓞ orcid.org/0000-0002-3607-3426; Email: orrit@physics.leidenuniv.nl

Authors

Xuxing Lu − *Huygens-Kamerlingh Onnes Laboratory, Leiden University, 2300 RA Leiden, Netherlands;* ⓞ orcid.org/0000-0002-1385-1563

Gang Ye − *Stratingh Institute for Chemistry, Zernike Institute for Advanced Materials, University of Groningen, 9747 AG Groningen, Netherlands*

Deep Punj − *Huygens-Kamerlingh Onnes Laboratory, Leiden University, 2300 RA Leiden, Netherlands;* ⓞ orcid.org/0000-0003-3976-262X

Complete contact information is available at:
https://pubs.acs.org/10.1021/acsphotonics.0c00803

Author Contributions

M.O. designed the study. X.L. performed the simulations and optical measurements. R.C. and G.Y. designed the NDI-2TEG-3T dyes and G.Y. synthesized the dyes. X.L., D.P., and M.O. wrote the manuscript. All authors read, discussed, and corrected the manuscript.

Notes

The authors declare no competing financial interest.

■ ACKNOWLEDGMENTS

■ REFERENCES

(1) Zander, C.; Enderlein, J.; Keller, R. A. *Single-Molecule Detection in Solution: Methods and Applications*; VCH-Wiley, 2002.

(2) Lu, G.; Zhang, T.; Li, W.; Hou, L.; Liu, J.; Gong, Q. Single-Molecule Spontaneous Emission in the Vicinity of an Individual Gold Nanorod. *J. Phys. Chem. C* **2011**, *115*, 15822−15828.

(3) Ho, W. Single-molecule chemistry. *J. Chem. Phys.* **2002**, *117*, 11033−11061.

(4) Garoli, D.; Yamazaki, H.; Maccaferri, N.; Wanunu, M. Plasmonic Nanopores for Single-Molecule Detection and Manipulation: Toward Sequencing Applications. *Nano Lett.* **2019**, *19*, 7553−7562.

(5) Barulin, A.; Claude, J.-B.; Patra, S.; Bonod, N.; Wenger, J. Deep Ultraviolet Plasmonic Enhancement of Single Protein Autofluorescence in Zero-Mode Waveguides. *Nano Lett.* **2019**, *19*, 7434−7442.

(6) Moerner, W. E.; Kador, L. Optical detection and spectroscopy of single molecules in a solid. *Phys. Rev. Lett.* **1989**, *62*, 2535−2538.

(7) Moerner, W. E.; Orrit, M. Illuminating Single Molecules in Condensed Matter. *Science* **1999**, *283*, 1670−1676.

(8) Moerner, W. E. W. E. Nobel Lecture: Single-molecule spectroscopy, imaging, and photocontrol: Foundations for super-resolution microscopy. *Rev. Mod. Phys.* **2015**, *87*, 1183−1212.

(9) Orrit, M.; Bernard, J. Single pentacene molecules detected by fluorescence excitation in a p-terphenyl crystal. *Phys. Rev. Lett.* **1990**, *65*, 2716−2719.

(10) Ha, T. Single-Molecule Fluorescence Resonance Energy Transfer. *Methods* **2001**, *25*, 78−86.

(11) Keller, R. A.; Ambrose, W. P.; Goodwin, P. M.; Jett, J. H.; Martin, J. C.; Wu, M. Single-Molecule Fluorescence Analysis in Solution. *Appl. Spectrosc.* **1996**, *50*, 12A−32A.

(12) Moerner, W. E.; Fromm, D. P. Methods of single-molecule fluorescence spectroscopy and microscopy. *Rev. Sci. Instrum.* **2003**, *74*, 3597−3619.

(13) Anger, P.; Bharadwaj, P.; Novotny, L. Enhancement and Quenching of Single-Molecule Fluorescence. *Phys. Rev. Lett.* **2006**, *96*, 113002.

(14) Lakowicz, J. R. *Principles of Fluorescence Spectroscopy*; Springer Science & Business Media, 2013.

(15) Lichtman, J. W.; Conchello, J.-A. Fluorescence microscopy. *Nat. Methods* **2005**, *2*, 910−919.

(16) Chen, J.; Liu, W.; Zhou, B.; Niu, G.; Zhang, H.; Wu, J.; Wang, Y.; Ju, W.; Wang, P. Coumarin- and Rhodamine-Fused Deep Red Fluorescent Dyes: Synthesis, Photophysical Properties, and Bioimaging in Vitro. *J. Org. Chem.* **2013**, *78*, 6121−6130.

(17) Davies, M.; Jung, C.; Wallis, P.; Schnitzler, T.; Li, C.; Müllen, K.; Bräuchle, C. Photophysics of New Photostable Rylene Derivatives: Applications in Single-Molecule Studies and Membrane Labelling. *ChemPhysChem* **2011**, *12*, 1588−1595.

(18) Birks, J. B. *Organic Molecular Photophysics*; Wiley: New York, 1973; Vol. *1*, p 153.

(19) Prangsma, J. C.; Molenaar, R.; van Weeren, L.; Bindels, D. S.; Haarbosch, L.; Stouthamer, J.; Gadella, T. W. J.; Subramaniam, V.; Vos, W. L.; Blum, C. Quantitative Determination of Dark Chromophore Population Explains the Apparent Low Quantum Yield of Red Fluorescent Proteins. *J. Phys. Chem. B* **2020**, *124*, 1383−1391.

(20) Morozova, K. S.; Piatkevich, K. D.; Gould, T. J.; Zhang, J.; Bewersdorf, J.; Verkhusha, V. V. Far-Red Fluorescent Protein Excitable with Red Lasers for Flow Cytometry and Superresolution STED Nanoscopy. *Biophys. J.* **2010**, *99*, L13−L15.

(21) Shcherbakova, D. M.; Verkhusha, V. V. Near-infrared fluorescent proteins for multicolor in vivo imaging. *Nat. Methods* **2013**, *10*, 751−754.

(22) Kühn, S.; Håkanson, U.; Rogobete, L.; Sandoghdar, V. Enhancement of Single-Molecule Fluorescence Using a Gold Nanoparticle as an Optical Nanoantenna. *Phys. Rev. Lett.* **2006**, *97*, 017402.

(23) Ponzellini, P.; Zambrana-Puyalto, X.; Maccaferri, N.; Lanzano, L.; De Angelis, F.; Garoli, D. Plasmonic zero mode waveguide for highly confined and enhanced fluorescence emission. *Nanoscale* **2018**, *10*, 17362−17369.

(24) Khatua, S.; Paulo, P. M. R.; Yuan, H.; Gupta, A.; Zijlstra, P.; Orrit, M. Resonant Plasmonic Enhancement of Single-Molecule Fluorescence by Individual Gold Nanorods. *ACS Nano* **2014**, *8*, 4440−4449.

(25) Yuan, H.; Khatua, S.; Zijlstra, P.; Yorulmaz, M.; Orrit, M. Thousand-fold Enhancement of Single-Molecule Fluorescence Near a Single Gold Nanorod. *Angew. Chem., Int. Ed.* **2013**, *52*, 1217−1221.

(26) Khatua, S.; Yuan, H.; Orrit, M. Enhanced-fluorescence correlation spectroscopy at micro-molar dye concentration around a single gold nanorod. *Phys. Chem. Chem. Phys.* **2015**, *17*, 21127−21132.

(27) Punj, D.; Mivelle, M.; Moparthi, S. B.; van Zanten, T. S.; Rigneault, H.; van Hulst, N. F.; García-Parajó, M. F.; Wenger, J. A

plasmonic 'antenna-in-box' platform for enhanced single-molecule analysis at micromolar concentrations. *Nat. Nanotechnol.* **2013**, *8*, 512−516.

(28) Punj, D.; de Torres, J.; Rigneault, H.; Wenger, J. Gold nanoparticles for enhanced single molecule fluorescence analysis at micromolar concentration. *Opt. Express* **2013**, *21*, 27338−27343.

(29) Flauraud, V.; Regmi, R.; Winkler, P. M.; Alexander, D. T. L.; Rigneault, H.; van Hulst, N. F.; García-Parajo, M. F.; Wenger, J.; Brugger, J. In-Plane Plasmonic Antenna Arrays with Surface Nanogaps for Giant Fluorescence Enhancement. *Nano Lett.* **2017**, *17*, 1703−1710.

(30) Puchkova, A.; Vietz, C.; Pibiri, E.; Wünsch, B.; Sanz Paz, M.; Acuna, G. P.; Tinnefeld, P. DNA Origami Nanoantennas with over 5000-fold Fluorescence Enhancement and Single-Molecule Detection at 25 μM. *Nano Lett.* **2015**, *15*, 8354−8359.

(31) Kinkhabwala, A.; Yu, Z.; Fan, S.; Avlasevich, Y.; Mullen, K.; Moerner, W. E. Large single-molecule fluorescence enhancements produced by a bowtie nanoantenna. *Nat. Photonics* **2009**, *3*, 654−657.

(32) Kinkhabwala, A. A.; Yu, Z.; Fan, S.; Moerner, W. E. Fluorescence correlation spectroscopy at high concentrations using gold bowtie nanoantennas. *Chem. Phys.* **2012**, *406*, 3−8.

(33) Zijlstra, P.; Paulo, P. M. R.; Orrit, M. Optical detection of single non-absorbing molecules using the surface plasmon resonance of a gold nanorod. *Nat. Nanotechnol.* **2012**, *7*, 379−382.

(34) Vigderman, L.; Khanal, B. P.; Zubarev, E. R. Functional Gold Nanorods: Synthesis, Self-Assembly, and Sensing Applications. *Adv. Mater.* **2012**, *24*, 4811−4841.

(35) Chen, H.; Shao, L.; Li, Q.; Wang, J. Gold nanorods and their plasmonic properties. *Chem. Soc. Rev.* **2013**, *42*, 2679−2724.

(36) Lakowicz, J. R. Radiative decay engineering 5: metal-enhanced fluorescence and plasmon emission. *Anal. Biochem.* **2005**, *337*, 171−194.

(37) Muskens, O. L.; Giannini, V.; Sánchez-Gil, J. A.; Gómez Rivas, J. Strong Enhancement of the Radiative Decay Rate of Emitters by Single Plasmonic Nanoantennas. *Nano Lett.* **2007**, *7*, 2871−2875.

(38) Carminati, R.; Greffet, J. J.; Henkel, C.; Vigoureux, J. M. Radiative and non-radiative decay of a single molecule close to a metallic nanoparticle. *Opt. Commun.* **2006**, *261*, 368−375.

(39) Canevet, D.; Sallé, M.; Zhang, G.; Zhang, D.; Zhu, D. Tetrathiafulvalene (TTF) derivatives: key building-blocks for switchable processes. *Chem. Commun.* **2009**, 2245−2269.

(40) Chen, Y.; Liang, X.; Yang, H.; Wang, Q.; Zhou, X.; Guo, D.; Li, S.; Zhou, C.; Dong, L.; Liu, Z.; Cai, Z.; Chen, W.; Tan, L. Strong Near-Infrared Solid Emission and Enhanced N-Type Mobility for Poly(naphthalene Diimide) Vinylene by a Random Polymerization Strategy. *Macromolecules* **2019**, *52*, 8332−8338.

(41) Johnson, P. B.; Christy, R. W. Optical Constants of the Noble Metals. *Phys. Rev. B* **1972**, *6*, 4370−4379.

(42) Dulkeith, E.; Morteani, A. C.; Niedereichholz, T.; Klar, T. A.; Feldmann, J.; Levi, S. A.; van Veggel, F. C. J. M.; Reinhoudt, D. N.; Möller, M.; Gittins, D. I. Fluorescence Quenching of Dye Molecules near Gold Nanoparticles: Radiative and Nonradiative Effects. *Phys. Rev. Lett.* **2002**, *89*, 203002.

(43) Cannone, F.; Chirico, G.; Bizzarri, A. R.; Cannistraro, S. Quenching and Blinking of Fluorescence of a Single Dye Molecule Bound to Gold Nanoparticles. *J. Phys. Chem. B* **2006**, *110*, 16491−16498.

(44) Vukovic, S.; Corni, S.; Mennucci, B. Fluorescence Enhancement of Chromophores Close to Metal Nanoparticles. Optimal Setup Revealed by the Polarizable Continuum Model. *J. Phys. Chem. C* **2009**, *113*, 121−133.

(45) Caldarola, M.; Pradhan, B.; Orrit, M. Quantifying fluorescence enhancement for slowly diffusing single molecules in plasmonic near fields. *J. Chem. Phys.* **2018**, *148*, 123334.

(46) Pradhan, B.; Khatua, S.; Gupta, A.; Aartsma, T.; Canters, G.; Orrit, M. Gold-Nanorod-Enhanced Fluorescence Correlation Spectroscopy of Fluorophores with High Quantum Yield in Lipid Bilayers. *J. Phys. Chem. C* **2016**, *120*, 25996−26003.

(47) Mooradian, A. Photoluminescence of Metals. *Phys. Rev. Lett.* **1969**, *22*, 185−187.

(48) Zhang, W.; Caldarola, M.; Lu, X.; Pradhan, B.; Orrit, M. Single-molecule fluorescence enhancement of a near-infrared dye by gold nanorods using DNA transient binding. *Phys. Chem. Chem. Phys.* **2018**, *20*, 20468−20475.